

PERFORMANCE ENHANCEMENT OF MAGNETIC BEADS-GRAPHENE OXIDE-TiO₂ COMPOSITE FILM ON ZnO NANOWIRES FOR DSSCs

Jung-Chuan Chou ^{1*}, Pei-Hong You ², Yi-Hung Liao ³, Chih-Hsien Lai ⁴, Chien-Hung Kuo ², Cheng-Chu Ko ⁵, and Yu-Hsun Nien ⁶

ABSTRACT

Dye-sensitized solar cells (DSSCs) were fabricated using photoanodes made from zinc oxide nanowires (ZNWs)/graphene oxide (GO) - titanium dioxide (TiO₂) composite film. In this study, we used magnetic beads (MBs) to modify double layer structure. DSSC based on ZNWs/MBs (0.25 mL)-GO-TiO₂ composite photoelectrode exhibited a high energy conversion efficiency (η) of 4.46%, compared with a DSSC based on ZNWs/GO-TiO₂ composite photoelectrode (3.53%), accompanied by increment short-circuit photocurrent. According to the experiment result, which could be attributed to the high specific surface area of MBs. The effects of GO and MBs for photovoltaic performances of the DSSC were investigated by field emission scanning electron microscopy (FE-SEM), solar simulator, UV-visible spectrometer and electrochemical impedance spectroscopy (EIS).

Keywords: Zinc oxide nanowire, titanium dioxide, dye-sensitized solar cell, graphene oxide, magnetic beads and electrochemical impedance spectroscopy.

1. INTRODUCTION

Dye-sensitized solar cells (DSSCs) are photoelectrochemical cell, which was first suggested by O'Regan and Grätzel in 1991. Dye-sensitized solar cells have been extensively studied as potential candidates for next-generation solar cells, because they have reasonable conversion efficiency, low cost, a simpler structure and lower fabrication cost than conventional silicon-based solar cells (O'Regan and Grätzel 1991; Chen 2016). However, the DSSCs are still facing several critical problems, such as short long life and recombination. Some researchers attempted to improve the properties of the TiO₂ electrode or used double layer structure, which can increase carrier lifetime and improve the photovoltaic conversion efficiency of DSSC (Rani and Tripathi 2016; Al-Juaid *et al.* 2013).

Because of their low cost, high porosity, wide bandgap and unique electrical properties, titanium dioxide (TiO₂) is widely used in various applications such as photocatalyst, dye sensitized solar cell, gas sensor, optical devices etc. (Xi *et al.* 2014; Zhang *et al.* 2015).

Manuscript received May 29, 2018; revised August 19, 2018; accepted September 23, 2018.

^{1*} Professor (corresponding author), Graduate School of Electronic Eng., National Yunlin University of Science and Technology, Douliou, Taiwan 64002, R.O.C. (e-mail: choujc@yuntech.edu.tw).

² Formerly Master student, Graduate School of Electronic Eng., National Yunlin University of Science and Technology, Taiwan R.O.C.

³ Associate Professor, Dept. of Information and Electronic Commerce Management, TransWorld University, Yunlin, Taiwan 64063, R.O.C.

⁴ Associate Professor, Graduate School of Electronic Eng., National Yunlin University of Science and Technology, Taiwan, R.O.C.

⁵ Master student, Graduate School of Electronic Eng., National Yunlin University of Science and Technology, Taiwan, R.O.C.

⁶ Professor, Graduate School of Chemical and Materials Eng., National Yunlin University of Science and Technology, Taiwan, R.O.C.

Because of its wide direct bandgap (3.37 eV) and high exciton binding energy (60 m eV), zinc oxide (ZnO) is an attractive material and has been investigated widely for applications in piezoelectric devices, sensor and solar cell etc.. The electron mobility is higher in ZnO than in TiO₂ and band gap is similar to TiO₂. On the other hand, the ZnO has various morphologies, such as nanoparticles, nanowires, nanotube and nanoflowers etc. (Chao *et al.* 2010; Manoharan *et al.* 2016; Xue *et al.* 2011).

In this paper, ZnO nanowires (ZNWs) were deposited by a water bath method to fabricate a DSSC. The main object of this paper is to optimize the ZnO structure, since electron transfer, suppressing of electron recombination and the electron diffusion of ZnO are expected to be more efficient (Rey *et al.* 2011).

Law *et al.* 2005 first demonstrated the capability of using vertical ZnO nanowire (NW) arrays in DSSCs. After that, other morphologies using ZnO nanostructures were improved the photovoltaic conversion efficiency, such as Yang *et al.* (2016) used hydrothermal method deposition to fabricate ZnO nanowires on the TiO₂ film, which made photovoltaic conversion efficiency of DSSC achieve 5.23%.

Graphene is a novel two-dimensional (2D) nanomaterial with exhibits low resistance, excellent optical transmittance and electron transport (Geim *et al.* 2009; Sun *et al.* 2011). As a result of its high mobility up to $10^6 \text{ cm}^2 \text{ V}^{-1} \text{ s}^{-1}$ (Bonaccorso *et al.* 2010), high specific surface area reaching $2630 \text{ m}^2 \text{ g}^{-1}$, tunable band gap and high mechanical strength, graphene should be an ideal material in DSSC photoanode.

Magnetic beads (MBs) were composed of Fe₃O₄, which have been widely used in the biomedical fields because of its high specific surface area, biocompatibility, and good dispersion (Nouira *et al.* 2013; Chou *et al.* 2016). Many researches about Fe₃O₄ are as a photocatalyst, which have been widely developed and could be used magnetic fields to influence electron transfer.

In this study, we used MBs to modify ZNWs/GO/TiO₂ composite film, which was prepared different MBs contents (0.25 mL ~ 1.25 mL) to formulate composite pastes. It is expected the incorporation of magnetic beads in photoanode may enhance the conversion efficiency of DSSC by reducing the charge recombination. In addition, the surface morphology and photovoltaic analysis of DSSC were characterized by field emission scanning electron microscopy (FE-SEM), UV-visible spectrometer (UV-vis), solar simulator, electrochemical impedance spectroscopy (EIS).

2. EXPERIMENTAL

2.1 Materials

The graphite powders were purchased from Enerage Inc., Taiwan. MBs solution was purchased from Quantum Biotechnology Inc., Taiwan. The titanium dioxide powders (P25) and ruthenium-535 (N₃) were manufactured from UniRegion Bio-Tech, Taiwan. The zinc acetate was purchased from J. T. Baker, United States. The hexamethylenetetramine was purchased from Alfa Aesar, United States. The iodine puriss (I₂) was purchased from Riedel-de Haën, Germany. The ethanol was purchased from Katayama Chemical, Japan. The Triton X-100 was purchased from PRS Panteac, Spain. The acetylacetone (AcAc), lithium iodide (LiI) and 4-Tert-Butylpyridine (TBP) were purchased from Sigma-Aldrich, United States. The 1-propyl-2, 3-dimethylimidazolium iodide (DMPII) was purchased from Tokyo Chemical, Japan.

2.2 Synthesis of the Graphene Oxide

GO was prepared by the modified Hummer's method (Shen *et al.* 2009). Typically, graphite/sodium nitrate (NaNO₃) (vol. ratio: 1/1) and sulfuric acid (H₂SO₄) were stirred in an ice bath for 1 hour, and then KMnO₄ was slowly added. The solution was stirred for 48 hours. The obtained product was washed using a mixed solution of hydrochloric acid (HCl)/H₂O (vol. ratio: 1/10). Finally, the precipitation was washed using D. I. water until the pH 7.0, and freeze-dried to remove water to obtain brown graphene oxide powder (Chou *et al.* 2016).

2.3 Fabrication of the ZNWs/MBs-GO-TiO₂ Composite Layer for Dye-Sensitized Solar Cell

The photoelectrode of DSSC consists of a MBs-GO-TiO₂ composite layer and a ZNWs layer. The cleaned FTO was stucked with the teflon tape on the conducting surface to define the active area (8 mm × 8 mm). The ZnO seed was fabricated by the radio frequency (R.F.) sputtering system. A ZnO target with a purity of 99.99 % was sputtered in a reactive gas mixture of Ar and O₂ with a pressure flow ratio Ar/O₂ of 9/1 (sccm). The R. F. power, working pressure and deposited time were set 60 W, 3 mTorr and 5 min, respectively. Then, ZNWs were fabricated by the water bath method. The growth solution contained 1.1 g zinc acetate, 0.7 g hexamethylenetetramine and 500 mL D. I. water for 2 hours. The temperature of ZnO nanowires deposition was set 90 °C. And then, the MBs-GO-TiO₂ colloid consists of 3 g TiO₂ powders (P25), 0.15 mL Triton X-100, 0.05 mL AcAc, 0.15 mL graphene oxide and different concentrations of MBs solution (0.25 mL ~ 2.5 mL), which were mixed by a magnetic stirrer for 24 hr. The colloid was

fabricated on ZNWs photoanode by the spin coating method. After that, the active area of photoelectrode was set 0.64 cm². The photoelectrode was annealed at 450°C for 30 min, then the photoelectrode was immersed in the 3 × 10⁻⁴ M N3 dye for 24 hr. Finally, the photoelectrode, Pt-counter electrode and electrolyte were assembled into a sandwich structure as shown in Fig. 1.

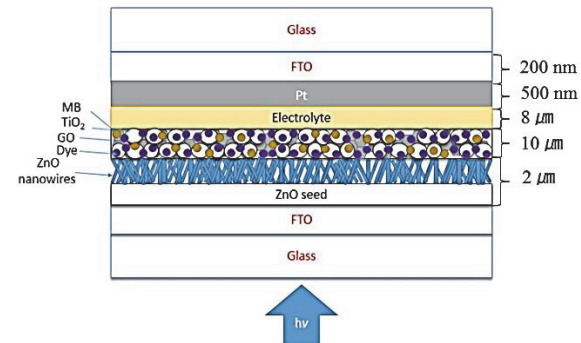


Fig. 1 The structure of DSSC with MBs-GO-TiO₂ composite and ZNWs layer

2.4 Characteristic and Photoelectric Properties of the ZNWs/MBs-GO-TiO₂ Composite Film

The surface morphologies of ZNWs were analyzed by FE-SEM (Hitachi S4800-I, Japan). The absorption spectra of the photoelectrode was measured by using UV-vis spectrophotometer (Jacomodel V-600, Taiwan). The thickness of the photoanode films was measured by a surface profiler (Bruker DektakXT, USA). The photovoltaic parameters of DSSC were measured by a solar simulator (MFS-PV-Basic-HMT, Taiwan) at AM 1.5G (100 mW/cm²). The electrochemical property of DSSC was measured by an electrochemical impedance analyzer (BioLogic SP-150, France). Besides, impedance measurement of cells was recorded over a frequency range of 1 MHz to 50 mHz with an AC amplitude of 10 mV.

3. RESULTS AND DISCUSSION

3.1 Synthesis of the ZnO Nanowires Composite Film

The ZnO nanowires were synthesized using water bath method followed by annealing in air. It can be observed in the SEM image. Figure 2 showed the cross-section SEM image of ZnO nanowires. The ZnO nanowires were grown on the ZnO seed substrate, and an average length of nanowires is 511 nm. Moreover, the diameter of nanowires is 46 nm.

3.2 Specific Surface Areas of the Different Composite Film

The comparsion of specific surface areas for different composite films are shown in Table I. The specific surface area of the MBs-GO-TiO₂/ZnO nanowires composite film was measured by Brunner-Emmet-Teller (BET) Sorptometer (BET-201A), and which was 214.2 m² g⁻¹. Compared with other literatures (Sofiane *et al.* 2016; Jadhav 2014; Zhang *et al.* 2015; Fang *et al.* 2015), the MBs-GO-TiO₂/ZnO nanowires exhibited a larger surface area, which could be attributed to the the high specific surface area of GO and MBs.

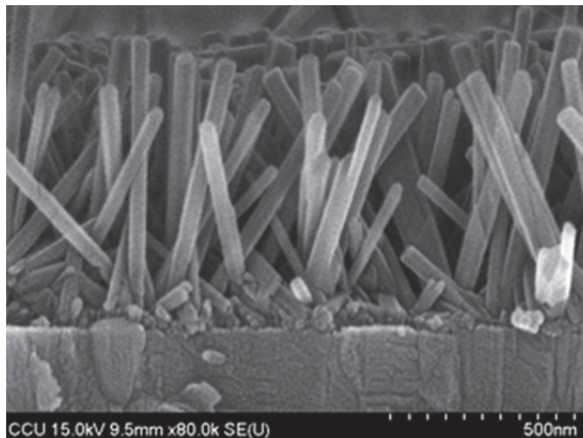


Fig. 2 The SEM image of cross section view for ZnO nanowires

3.3 Dye Adsorption of the Different Composite Films

In order to find out the reason for higher short-circuit current density (J_{sc}) of the composite film, both ZnO, ZnO nanowires/TiO₂, ZnO nanowires/GO-TiO₂ and ZnO nanowires/MBs-GO-TiO₂ photoanodes were immersed 0.1 M NaOH solutions to desorb the N3 dye from the active area of photoelectrode. Figure 3 showed UV-Vis absorbance spectra of the dye solution. The absorbance peaks were observed at 380 nm and 500 nm for N3 dye, and the loading of dye adsorption was shown in Table II. From the UV-Vis absorbance spectra, ZnO nanowires/MBs-GO-TiO₂ composite film showed better absorbance than other composite films. However, the experimental results could be attributed that the GO had high specific surface area, and MBs had good dispersion. In general, more dye loading could obtain more electron-hole pair under the incidence for photoanodes, which can improve J_{sc} (Marimuthu *et al.* 2017).

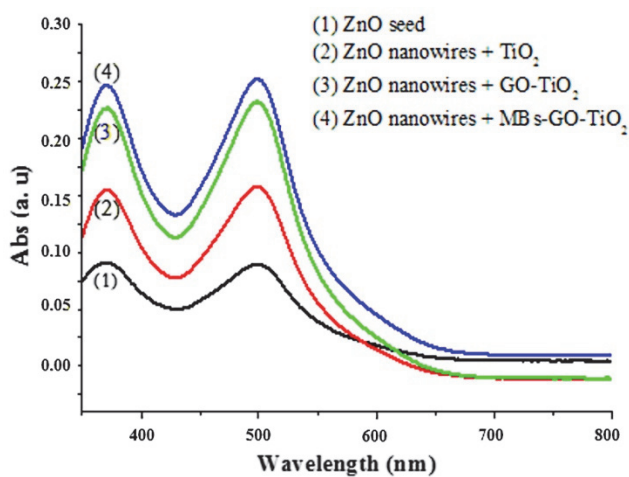


Fig. 3 The UV-Vis absorbance spectra of the different composite films

3.4 Effect of the Different Magnetic Beads Contents for Photovoltaic Parameters

Figure 4 showed the current density-voltage (J-V) curves of the ZNWS/GO-TiO₂ based on different magnetic beads solutions

(0.25, 0.50, 0.75, 1.00, 1.25 mL) in ZNWS/MBs-GO-TiO₂. The corresponding performance parameters are summarized in Table II. The open-circuit voltages (V_{oc}) of the five samples show the nearly of 0.75 V, which could be attributed DSSC composed of the ZNWS/MBs-GO-TiO₂ as the working electrode and Pt films as the counter electrode. The fill factor of the samples are almost similar, but the short-circuit current density (J_{sc}) are different. The J_{sc} is a key parameter to enhance the photovoltaic conversion efficiency. Moreover, the J_{sc} means the output current density of DSSC when output voltage is zero. The photovoltaic conversion efficiency of the ZNWS/MBs (0.50 mL)-GO-TiO₂ is higher than other MBs solutions. Because the appropriate concentration of MBs can ideally accelerate the transition for photo-generated electron from TiO₂ to FTO before recombination. Interestingly, the performances of DSSCs are greatly improved by incorporating magnetic beads into DSSC. A higher J_{sc} of 11.38 mA cm⁻² with photovoltaic conversion efficiency (η) of 4.46% are observed, and the increase for the η and J_{sc} reach 26% and 33%, respectively. According to our experimental result, this could be attributed that the MBs have high specific surface area and good charge transfer (Chou *et al.* 2016).

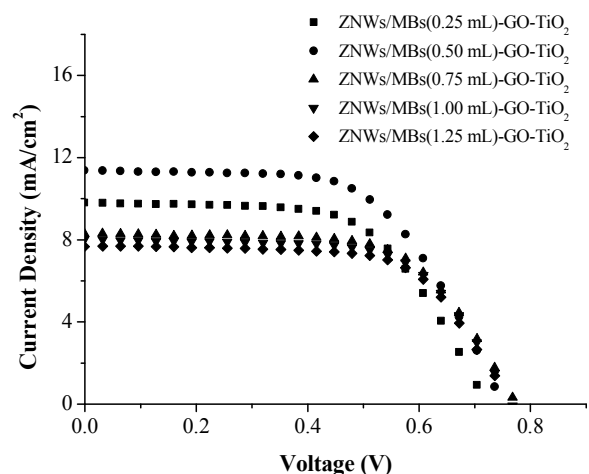


Fig. 4 The J-V curves of DSSCs with different magnetic beads solutions in photoanodes

Table 1 Comparison of specific surface areas, diameters, and length for different composite films

Structure	Specific surface areas (m ² /g)	Reference
ZnO nanowires	171.1	In this study
TiO ₂ (P25)	054.1	In this study
GO-TiO ₂ /ZnO nanowires	208.8	In this study
MBs-GO-TiO ₂ /ZnO nanowires	214.2	In this study
TiO ₂ (P25)	052.1	Sofiane <i>et al.</i> 2016
ZnO nanowires	151.1	Jadhav <i>et al.</i> 2014
TiO ₂ nanowires	080.0	Zhang <i>et al.</i> 2015
Ag nanowires	009.5	Fang <i>et al.</i> 2015

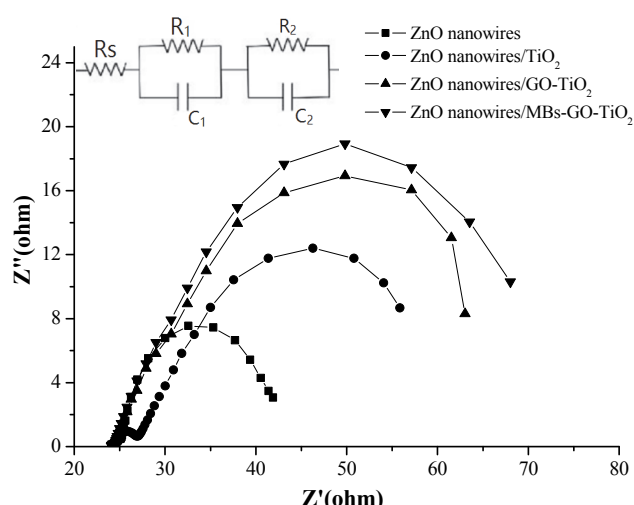
Table 2 The photovoltaic parameters of DSSCs with different magnetic beads solutions in ZNWs/MBs-GO-TiO₂

Structure	Adsorbed dye (mol/cm ² × 10 ⁻⁸)	V _{oc} (V)	J _{sc} (mA cm ⁻²)	F. F. (%)	η (%)
ZNWs	4.58	0.38	0.44	39.25	0.10
ZNWs/TiO ₂	7.44	0.73	7.73	57.47	3.23
ZNWs/GO-TiO ₂	10.84	0.72	8.57	56.90	3.53
ZNWs/MBs (0.25 mL) -GO-TiO ₂	N/A	0.74	9.82	60.61	4.28
ZNWs/MBs (0.50 mL) -GO-TiO ₂	12.48	0.76	11.38	64.83	4.46
ZNWs/MBs (0.75 mL) -GO-TiO ₂	N/A	0.77	8.32	63.91	4.10
ZNWs/MBs (1.00 mL) -GO-TiO ₂	N/A	0.76	8.02	64.63	3.98
ZNWs/MBs (1.25 mL) -GO-TiO ₂	N/A	0.75	7.77	65.80	3.84

N/A: Not available

3.5 Effect of Different Magnetic Beads for Internal Impedances

Figure 5 showed the Nyquist plots and equivalent circuit model of DSSCs modified by GO and MBs. semicircles in the Nyquist plots, R_s is the starting series resistance between the FTO glass and wires. The first semicircle represented charge-transfer resistance and interfacial capacitance between electrolyte and Pt-counter electrode (R₁ and C₁). The second semicircle represented recombination resistance and chemical capacitance at the interface of TiO₂/electrolyte (R₂ and C₂). Therefore, the resistance and capacitance parameters of equivalent circuit were summarized in Table III. The recombination impedance was increased from 38.70 Ω to 43.70 Ω when GO and MBs were modified in DSSC, which had the larger second semicircle, indicating the electron recombination resistance between TiO₂ and electrolyte is increased by introducing MBs (Tiana *et al.* 2011).

**Fig. 5** The Nyquist plots of DSSCs with different composite films**Table 3** The electrochemical impedance parameters of DSSC with different composite films

Structure	R ₁ (Ω)	C ₂ (mF)	R ₂ (Ω)	τ _n (Ω)
ZnO nanowires	0.29	0.75	17.40	13.05
ZnO nanowires/TiO ₂	2.60	1.21	28.92	34.99
ZnO nanowires/GO-TiO ₂	0.31	1.47	38.70	56.88
ZnO nanowires/MBs-GOTiO ₂	0.35	1.52	43.70	66.42

4. CONCLUSIONS

In this study, introducing MBs into ZnO nanowires/GO-TiO₂ based DSSC could effectively enhance the photocurrent, open-circuit voltage and fill factor. Thus the overall conversion efficiency could be improved due to the MBs high specific surface area and good charge transfer. When 0.5 mL MB was incorporated into ZNWs/GO-TiO₂ photoelectrode, DSSC showed the best performances with the higher J_{sc} of 11.38 mA cm⁻² and η of 4.46%.

ACKNOWLEDGMENTS

This work was supported by the Ministry of Science and Technology, Republic of China, under contract MOST 105-2221-E-224-049 and MOST 106-2221-E-224-047.

REFERENCES

- Al-juaid, F., Merazga, A., Al-Baradi, A., and Abdel-wahab, F. (2013). "Effect of sol-gel ZnO spin-coating on the performance of TiO₂-based dye-sensitized solar cell." *Solar Energy Materials and Solar Cells*, **87**, 98-103.
- Bai, X., Yi, L., Liu, D., Nie, E., Sun, C., Feng, H., Xu, J., Jin, Y., Jiao, Z., and Sun, X. (2011). Electrodeposition from ZnO nano-rods to nano-sheets with only zinc nitrate electrolyte and its photoluminescence, *Applied Surface Science*, **257**, 10317-10321.
- Bonaccorso, F., Sun, Z., Hasan, T., and Ferrari, A.C. (2010). "Graphene photonics and optoelectronics." *Nature Photonics*, **4**, 611-622.
- Chao, C.H., Chang, C.L., Chan, C.H., Lien, S.Y., Weng, K.W., and Yao, K.S. (2010). Rapid thermal melted TiO₂ nano-particles into ZnO nano-rod and its application for dye sensitized solar cells, *Thin Solid Films*, **518**, 7209-7212.
- Chen, D.Y., Kao, J.Y., Hsu, C.Y., and Tsai, C.H. (2016). The effect of AZO and compact TiO₂ films on the performance of dye-sensitized solar cells." *Journal of Electroanalytical Chemistry*, **766**, 1-7.
- Chou, J.C., Chen, J.S., Liao, Y.H., Lai, C.H., Huang, M.S., Wu, T.Y., Zhuang, B.Y., Yan, S.J., Chou, H.T., and Hsu, C.C. (2016). "Effect of different contents of magnetic beads on enzymatic IGZO glucose biosensor." *Materials Letter*, **175**, 241-243.
- Chou, J.C., Chu, C.M., Liao, Y.H., Huang, C.H., Lin, Y.J., Wu, H., and Nien, Y.H. (2016). "The incorporation of graphene and magnetic beads into dye-sensitized solar cells and application with electrochemical capacitor." *IEEE Journal of Photovoltaics*, **6**, 223- 229.
- Chou, J.C., Huang, C.H., Lin, Y.J., Chu, C.M., Liao, Y.H., Tai, L.H., and Nien, Y.H. (2016). "The influence of different annealing temperatures on graphene-modified TiO₂ for dye-sensitized solar cell." *IEEE Transactions on Nanotechnology*, **15**, 164-170.

- Fang, X., Ding, Q., Fan, L.W., Lu, H., and Yu, Z.T. (2015). "Effects of inclusion size on thermal conductivity and rheological behavior of ethylene glycol-based suspensions containing silver nanowires with various specific surface areas." *International Journal of Heat and Mass Transfer*, **81**, 554-562.
- Geim, A.K. (2009). "Graphene: Status and Prospects." *Science*, **324**, 1530-1534.
- Jadhav, N.A., Singh, P.K., Rhee, H.W., and Bhattacharya, B. (2014). "Effect of variation of average pore size and specific surface area of ZnO electrode (WE) on efficiency of dye-sensitized solar cells." *Nanoscale Research Letters*, **9**, 1-8.
- Law, M., Greene, L.E., Johnson, J.C., Saykally, R., and Yang, P.D. (2005). "Nanowire dye-sensitized solar cells." *Nature Materials*, **4**, 455-459.
- Manoharan, C., Dhanapandian, S., and Arunachalam, A.M. (2016), "Bououdina, Physical properties of spray pyrolyzed nano flower ZnO thin films." *Journal of Alloys and Compounds*, **685**, 395-401.
- Marimuthu, T., Anandhan, N., Thangamuthu, R., and Surya, S. (2017). "Facile growth of ZnO nanowire arrays and nanoneedle arrays with flower structure on ZnO-TiO₂ seed layer for DSSC applications." *Journal of Alloys and Compounds*, **693**, 1011-1019.
- Nouira, W., Maaref, A., Elaissari, H., Vocanson, F., Siadat, M., and Jaffrezic-Renault, N. (2013). Comparative study of conductometric glucose biosensor based on gold and on magnetic nanoparticles." *Materials Science and Engineering*, **33**, 298-303.
- O'Regan, B. and Grätzel, M. (1991). "A low-cost, high-efficiency solar cell based on dye-sensitized colloidal TiO₂ films." *Nature*, **353**, 737-740.
- Rani, M. and Tripathi, S.K. (2016). "Electron transfer properties of organic dye sensitized ZnO and ZnO/TiO₂ photoanode for dye sensitized solar cells." *Renewable Sustainable Energy Rev.*, **61**, 97-107.
- Rey, G., Doisneau, B., Roussel, H., Deshayes, R., Consonni, V., Ternon, C., and Bellet, D. (2011). "Fabrication and characterization of a composite ZnO semiconductor as electron transporting layer in dye-sensitized solar cells." *Materials Science and Engineering B*, **176**, 653-659.
- Shen, J., Hu, Y., Shi, M., Lu, X., Chen, Q., Chen, L., and Ye, M. (2009). "Fast and facile preparation of graphene oxide and reduced graphene oxide nanoplatelets." *Chemistry of Materials*, **21**, 3514-3520.
- Sofiane, S. and Bilel, M. (2016). "Effect of specific surface area on photoelectrochemical properties of TiO₂ nanotubes, nanosheets and nanowires coated with TiC thin films." *Journal of Photochemistry and Photobiology A: Chemistry*, **324**, 126-133.
- Sun, Y., Wu, Q., and Shi, G. (2011). "Graphene based new energy materials." *Energy & Environmental Science*, **4**, 11-13.
- Tiana, Y., Hua, C., Wu, Q., Wu, X., Li, X., and Hashim, M. (2011). "Investigation of the fill factor of dye-sensitized solar cell based on ZnO nanowire arrays." *Applied Surface Science*, **258**, 321-326.
- Xi, M., Zhang, Y., Long, L., and Li, X. (2014). Controllable hydrothermal synthesis of rutile TiO₂ hollow nanorod arrays on TiCl₄ pretreated Ti foil for DSSC application." *Journal of Solid State Chemistry*, **219**, 118-126.
- Yang, Y., Zhao, J., Cui, C., Zhang, Y., Hu, H., Xu, L., Pan, J., Li, C., and Tang, W. (2016). "Hydrothermal growth of ZnO nanowires scaffolds within mesoporous TiO₂ photoanodes for dye-sensitized solar cells with enhanced efficiency." *Electrochimica Acta*, **196**, 348-356.
- Zhang, P., Fujitsuka, M., and Majima, T. (2015). "TiO₂ mesocrystal with nitrogen and fluorine codoping during topochemical transformation: Efficient visible light induced photocatalyst with the codopants." *Applied Catalysis B*, **185**, 181-188.
- Zhang, Y., Han, C., Zhang, G., Dionysiou, D.D., and Nadagouda, M.N. (2015). "PEG-assisted synthesis of crystal TiO₂ nanowires with high specific surface area for enhanced photocatalytic degradation of atrazine." *Chemical Engineering Journal*, **268**, 170-179.

